Available online at www.sciencedirect.com
SCIENCE DIRECT®
Thermochimica Acta 427 (2005) 155–161
thermochimica acta
www.elsevier.com/locate/tca

Decomposition of mixed Mn and Co nitrates supported on carbon

Terhi Nissinen[a,*], Markku Leskelä[b], Michael Gasik[a], Jaakko Lamminen[c]

[a] *Laboratory of Materials Processing and Powder Metallurgy, Helsinki University of Technology, P.O. Box 6200, FI-02015 HUT, Finland*
[b] *Department of Chemistry, Laboratory of Inorganic Chemistry, P.O. Box 55, FI-00014 University of Helsinki, Finland*
[c] *Laboratory of Applied Thermodynamics, Helsinki University of Technology, P.O. Box 4400, FI-02015 HUT, Finland*

Received 6 July 2004; received in revised form 6 September 2004; accepted 9 September 2004
Available online 19 October 2004

Abstract

The effect of varying amounts of carbon support on the decomposition of mixed Mn and Co nitrates and the formation of spinel $MnCo_2O_4$ is studied in this work. The molar ratios of the studied samples were n(Mn):n(Co):n(NO_3^-):n(C) = 1:2:6:Y and Y was varied from 0 to 25. IR and XRD measurements of the samples heated at various temperatures revealed spinel formation from the pure nitrates at 240 °C but from the supported nitrates (Y = 15) already at 160 °C. The spinel prepared from pure nitrates at temperatures ≤400 °C was clearly non-stoichiometric. The supported nitrates produced a less non-stoichiometric spinel with smaller crystallite size. TG measurements revealed that compared with the pure nitrates, the decomposition of the supported nitrates initiated and was completed at lower temperatures. When carbon content was increased from Y = 0 to 20, the onset of the nitrate decomposition was shifted to lower temperatures. The increase of carbon amount beyond Y = 20 did not result in any considerable change. The decomposition of the supported nitrates was completed at temperatures 50–70 °C lower than the pure nitrates. Both the decomposition of nitrates and the presence of spinel oxide enhanced the oxidation of carbon.

Keywords: $MnCo_2O_4$; Carbon; Supported nitrates; Thermogravimetry; Decomposition gases

1. Introduction

An interesting and feasible way to prepare small metal oxide particles is to use carbon as a support for nitrate precursors [1–4]. Our interest has been focused on the preparation of spinel $MnCo_2O_4$, which has several applications, for instance as catalysts for decomposition of NO and CO [5], reduction of nitrogen oxides into N_2 [6], and oxygen reduction reaction [3,4,7,8]. For optimal preparation conditions it is essential to know what factors affect the decomposition of the nitrate precursors. No detailed information on the decomposition of the mixed Mn–Co nitrates was found in the literature, but several reports for both the Mn and Co nitrates exist. Different decomposition temperatures, mechanisms, and intermediates are reported for the Mn and Co nitrates, depending on factors such as heating rate, moisture content of the atmosphere [9], hydration degree of the nitrates [10], crystal size and support [11], and the sample mass and the diameter of the crucibles used in the measurements [10].

In air or oxygen manganese nitrate decomposes up to 200–220 °C [10–14], and cobalt nitrate up to 240–280 °C [11,12,15–17]. The decomposition of the nitrates can occur simultaneously or after the water evaporation and its mechanism can be rather complicated. Transition metal nitrates usually dehydrate below 180 °C followed by the decomposition of the anhydrous nitrate below 280 °C [12]. Mn [10] and Co [11] nitrates have been reported to first lose water followed by the decomposition of the anhydrous nitrate, but also simultaneous water evaporation and nitrate decomposition for Co-nitrate has been reported [17]. Formation of different unstable intermediates has been reported, such as $MnO_{1.2}(NO_3)_{0.8}$ [13], $MnONO_3$ [9], $Co_2(NO_3)_2(OH)_2$, $CoO{\cdot}CoONO_3$, Co_2ONO_3 [14], and CoO and Co_2O_3 [17].

In moist atmosphere the decomposition of the nitrates can occur at lower temperatures than in dry atmosphere [9]. More-

* Corresponding author. Tel.: +358 9 451 2777; fax: +358 9 451 2799.
E-mail address: terhi.nissinen@hut.fi (T. Nissinen).

0040-6031/$ – see front matter © 2004 Elsevier B.V. All rights reserved.
doi:10.1016/j.tca.2004.09.005

over, hydrated Mn nitrate has been reported to decompose at lower temperatures than nearly dehydrated one [10]. The decomposition of supported nitrates can be strongly affected by the nature of the support. The results by Tiernan et al. [15] show that, depending on the properties of the support, the decomposition of the supported cobalt nitrate can either be delayed or enhanced. Further, the crystal size of the nitrates can affect the decomposition; Cseri et al. [11] have reported that compared with the pure metal nitrates the decomposition of metal nitrates supported on a clay started and was completed at 0–40 and 5–105 °C lower temperatures, respectively. Since the decomposition shifted to lower temperatures pronouncedly for the most amorphous nitrates, it was expected that this shift was due to the small crystal size of the nitrates. They also note that some decomposition steps that were observed during the decomposition of pure nitrates were not observed for the supported samples. The effect of varying amounts of carbon support on the decomposition of the mixed Mn and Co nitrates to form spinel $MnCo_2O_4$ is studied in this report.

2. Experimental

The molar ratios of the studied samples were n(Mn):n(Co):n(NO_3^-):n(C) = 1:2:6:Y. Samples with $Y = 0$ (no carbon), 5, 10, 15, 20, and 25, were prepared by dissolving analytical grade nitrates $Co(NO_3)_2{\cdot}6H_2O$ (Merck, 98.5%) and $Mn(NO_3)_2{\cdot}4H_2O$ (Merck, 99%) in water. Aqueous solutions of the nitrates were mixed with varying amounts of carbon powder (Ketjenblack® EC-300J, Akzo Nobel) having a specific surface area of 950 $m^2\,g^{-1}$. The samples were dried at 40 °C in air.

The formation of the gaseous species during heating of the nitrates was studied by thermogravimetry combined with Fourier transformed infrared (TG–FTIR). Mass loss was recorded by Perkin-Elmer Thermogravimetric Analyser TG7. The measurements were carried out in air. The sample masses were 22 ($Y = 0$) and 17 mg ($Y = 20$), and the heating rate was 10 K min^{-1}. The TG analyser was coupled by a heated transfer line to a 10 cm^3 gas cell and Perkin-Elmer System 2000 FTIR. The temperatures of the transfer line and the gas cell were 186 and 190 °C, respectively. FTIR measurements were made with resolution of 2 cm^{-1} and 16 scans per slice.

The effect of varying carbon content on the decomposition of the mixed Mn–Co nitrates was studied by thermogravimetry combined with differential scanning calorimetry (TG–DSC). The measurements were carried out in a Netzsch STA449C Jupiter analyser in air. The sample masses were 20–21 mg. While the heating rate of 10 K min^{-1} was found feasible for TG–FTIR measurements in order to receive well readable FTIR spectra, the heating rate of 5 K min^{-1} was used in TG–DSC measurements in order to get more detailed information on the decomposition steps.

The samples for infrared (IR) and powder X-ray diffraction (XRD) studies were prepared with carbon contents of $Y = 0$ and 15. The dried samples, 3 g for $Y = 0$ and 3.5 g for $Y = 15$, were heated in air from room temperature up to 400 °C, at temperatures just below or above the temperatures at which mass losses were observed in TG measurements, or at 50 °C intervals. Each temperature was held for 30 min. The crucibles containing the samples were covered with lids, which were loose enough to allow gas exhaust but which prevented loss of sample during the burning of carbon, which initiated below 300 °C. IR measurements were recorded with a Perkin-Elmer Spectrum GX with DTGS detector with resolution of 4 cm^{-1} and 64 scans, and the KBr pellets contained 0.2 wt.% of the sample. XRD patterns were taken with a Philips diffractometer with Cu Kα as a radiation source, using step size 0.02° and step time of 1 s.

3. Results

To be able to compare the results with varying amounts of carbon, all TG results are normalised. In the mass scale (Figs. 2,3 and 5), 100% corresponds to the mass of the weighed hydrated nitrates with molar ratios of n(Mn):n(Co):n(NO_3^-):n(H_2O) = 1:2:6:16. The composition of $MnCo_2O_4$ corresponds to 28.4%.

3.1. Formation of gaseous species during decomposition

Fig. 1 shows the FTIR spectra of the gaseous species developed during the heating of the sample with $Y = 20$. The strongest absorptions bands of NO_2 and CO_2 together with TG curves for samples $Y = 0$ and 20 are plotted in Fig. 2. During drying at 40 °C part of the original water has evaporated. That is why the mass of Mn–Co nitrate in the beginning of the measurement is <100%. For the supported nitrates the presence of carbon raises the starting point beyond 100%.

When Mn–Co nitrate ($Y = 0$) was heated in air, evaporation of water had maximum rate around 200 °C and ceased before 260 °C, which is before the maximum of NO_2 formation. The formation of NO_2 gas started soon above 200 °C, had maximum at 270 °C, and ceased around 300 °C. In the case of supported nitrates ($Y = 20$) the evaporation of water had maximum rate at 140 °C and continued up to 220 °C simultaneously with NO_2 formation, although started to slow down when NO_2 formation had reached the maximum. The formation of NO_2 started above 100 °C, had maximum at 190 °C and ceased around 230 °C. The comparison of samples $Y = 0$ and 20 reveals that for the supported nitrates the decomposition initiated, had maximum, and ceased 100, 80, and 70 °C earlier, respectively. While sample $Y = 0$ showed NO_2 formation with several steps, only one step was clearly observable for $Y = 20$. This kind of fusing of the steps for supported nitrates has been reported previously [11].

When carbon was studied alone with TG its burning did not start before 550 °C in air. However, it is known that the

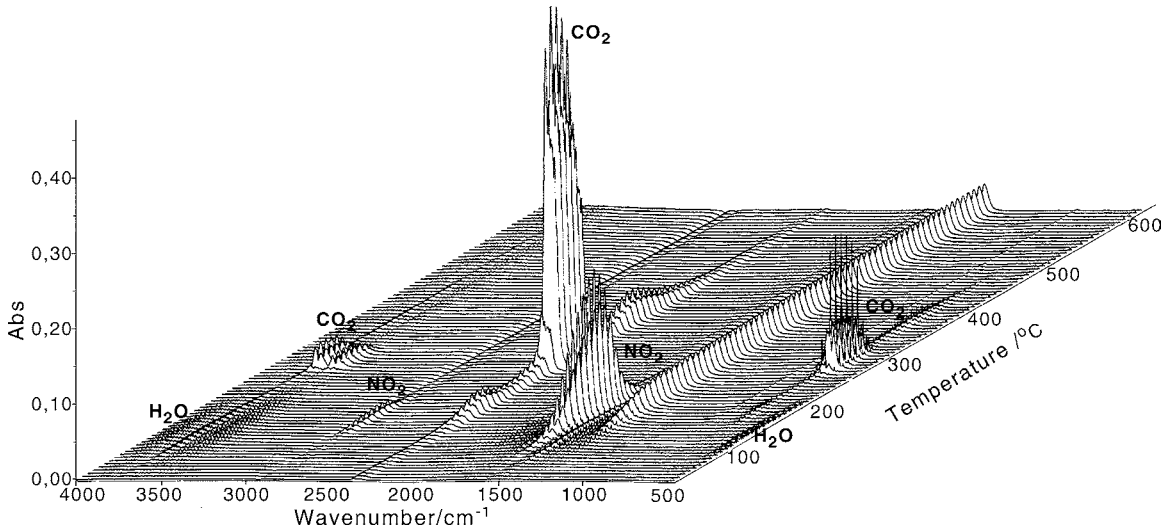

Fig. 1. FTIR spectra of gaseous species formed during heating of a supported Mn–Co nitrate with $Y = 20$, measured in air (10 K min^{-1}).

presence of metals and metal oxides or formation of nitrogen oxides can cause the oxidation of carbon at reasonably lower temperatures [1,18]. This was observed in this work as well. From the sample with $Y = 20$ the formation of CO_2 due to carbon oxidation started at 150 °C, had maximum at 300 °C, and ceased around 450 °C (Fig. 2). A local maximum of CO_2 formation at 200 °C was observed simultaneously with NO_2 formation (Fig. 2). The highest oxidation rate of carbon, observed at 300 °C, and another local maximum at 390 °C, are observed clearly after the nitrate decomposition. Hence, it can be concluded that both the Mn–Co nitrate decomposition and the presence of spinel oxide enhanced the carbon oxidation. When Mn–Co nitrate is impregnated into high surface area carbon powder, the materials seem to have a synergetic effect: first, carbon reduces the decomposition temperature of the nitrates, and second, the metal nitrates and oxides facilitate the oxidation of carbon.

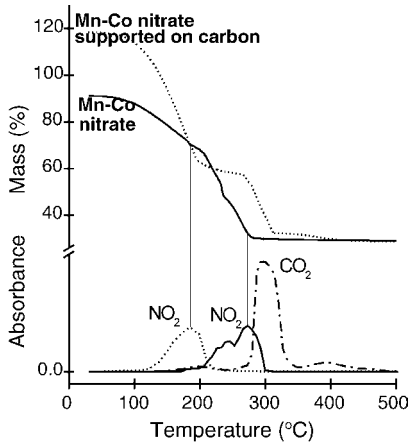

Fig. 2. Mass losses of the Mn–Co nitrate ($Y = 0$) and supported Mn–Co nitrate ($Y = 20$), measured in air (10 K min^{-1}), and the absorbance of IR bands for NO_2 and CO_2.

As Fig. 1 illustrates for $Y = 20$, the absorption band at 1380 cm^{-1} (and also a weak band at 834 cm^{-1}) is observable till the end of the measurement with its maximum intensity. This band appears soon after the onset of NO_2 formation, and its frequency is very close to N–O vibrations in NO_3^-. In the case of $Y = 0$ as well this band remained till the end of the measurement but was shifted to lower frequencies (1350–1370 cm^{-1}). While in the case of $Y = 20$ this band is clearly less intensive than NO_2 band (1630 cm^{-1}), in the case of $Y = 0$ it was clearly dominating being twice as intensive as the NO_2 band. Three additional absorptions at 890, 1712, and 3568 cm^{-1} were observed around the maximum formation of NO_2 only for the sample $Y = 0$. Thus, it seems that the composition of the NO_x gases is different for the pure nitrates and supported nitrates. Before and after each measurement the IR-window was cleaned, and it was noticed that during the measurement the colour of the window had turned from transparent to yellowish. These observations suggest that part of the reactants have evaporated in connection with the nitrate decomposition leading to the deposition of nitrates or the products of their partial decomposition on the IR window. Similarly, Nohman et al. [13] made IR gas phase analysis of various manganese complexes and noted that analysis of manganese nitrate was very difficult to perform owing to technical difficulties arising from the brown colored gases of nitrogen oxides.

3.2. The effect of varying amounts of carbon

Although the prepared samples were dried at 40 °C simultaneously for equally long time, the observations based on sample mass recorded before and after drying showed that the water content of the samples was not equal but varied depending on the carbon content. After drying, the water contents of the samples decreased almost linearly with the increase in carbon content. Moreover, during weighing

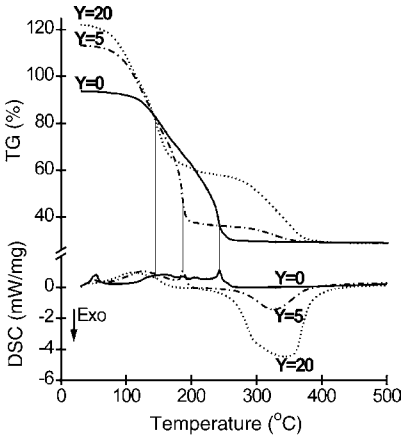

Fig. 3. TG and DSC curves of Mn–Co nitrate supported on varying amounts of carbon, measured in air (5 K min^{-1}).

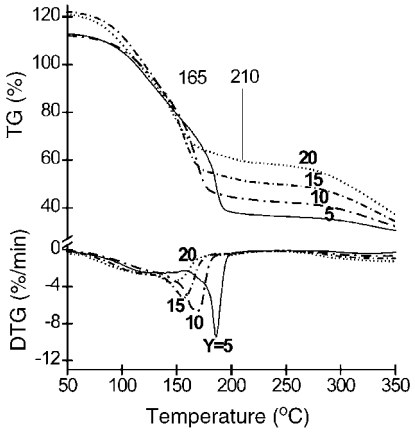

Fig. 5. TG and DTG curves of Mn–Co nitrate supported on varying amounts of carbon, measured in air (5 K min^{-1}).

of samples for the thermogravimetric measurements, the samples either lost or absorbed moisture rapidly depending on the prevailing humidity of air. As the molar ratios of the metal ions, nitrate and carbon were known, the water contents of the samples were determined from the thermogravimetric data by assessing that the composition of the samples is very close to $MnCo_2O_4$ at 700–900 °C. In the beginning of the TG-DSC measurements, the samples where n(Mn):n(Co):n(NO_3^-):n(C):n(H_2O) = 1:2:6:Y:Z with Y = 0, 5, 10, 15, and 20 were estimated to have water contents $Z \approx$ 13, 19, 15, 16, and 13, respectively. The TG–FTIR samples with Y = 0 and 20 were assessed to have water contents $Z \approx$ 12 and 10, respectively, in the beginning of the measurements.

Figs. 3–5 show the TG, DSC, and DTG curves of Mn–Co nitrate supported on varying amounts of carbon. Figs. 3 and 4 illustrate that the sample Y = 0 decomposes with several steps showing endothermic DSC peaks. The peak around 50 °C is attributed to melting. The observations from TG–FTIR measurements suggest that the peak at 160 °C would be attributed to water evaporation. The peaks between 180 and 210 °C are probably associated with the simultaneous water evaporation and nitrate decomposition, and the last peak at 240 °C to the decomposition of anhydrous nitrate. Mass loss calculations indicated that nitrates were mostly decomposed very soon after this step, around 260 °C.

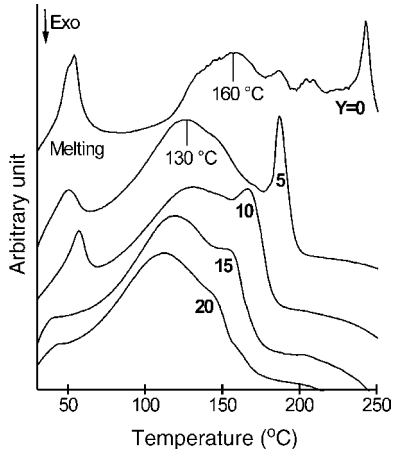

Fig. 4. DSC curves of Mn–Co nitrate supported on varying amounts of carbon, measured in air (5 K min^{-1}). At 30 °C, each curve has the value about 0 mW/mg. The curves have been lifted vertically to ensure the readability.

For the sample with Y = 5, DSC curve (Fig. 4) displays three endothermic peaks at 50, 130, and 185 °C. Again, the peak at 130 °C can be attributed to water evaporation and the peak at 185 °C to the decomposition of the anhydrous nitrate. Mass loss calculations indicated that nitrates were mainly decomposed fairly soon after the latter peak, slightly above 200 °C. The slow mass loss after the nitrate decomposition (Fig. 3) is probably attributed to slow oxidation of carbon. The mass loss due to clearly exothermic carbon oxidation initiates around 280 °C, has maximum at 330 °C and continues up to 400 °C.

Sample Y = 10 decomposed showing broad endothermic DSC peaks at 130 and 165 °C (Fig. 4). For samples Y = 15 and 20 the latter peaks become still broader and are shifted to lower temperatures. For Y = 20 the two peaks are nearly fused together, indicating that water evaporation and nitrate decomposition occur mostly simultaneously. The samples with $Y \geq$ 10 display an additional mass loss step (Fig. 5) initiating at 165–180 °C (depending on carbon content) and continuing up to 210 °C. TG–FTIR measurements (Fig. 2) show weak CO_2 formation together with NO_2 formation during this step up to 230 °C (the delay by 20° is due to higher heating rate). These data indicate that nitrates in the samples with $Y \geq$ 10 decompose first with simultaneous evaporation of water and then with simultaneous oxidation of carbon. The mass loss due to carbon combustion initiates at 260–280 °C (Figs. 3 and 5), has maximum around 330 °C, and continues up to 400–450 °C, the longer the higher the carbon content.

Fig. 6 shows the temperatures of the maximum mass loss rates attributed to nitrate decomposition, observed in DTG (Fig. 5). The shifting of the maximum mass losses to lower

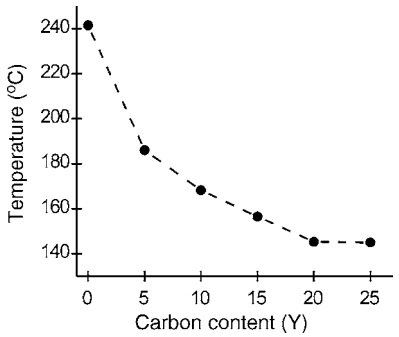

Fig. 6. Peak positions of maximum mass loss rate vs. carbon molar content *Y*, taken from the DTG data (Fig. 5).

temperatures is almost linear as Y increases from 5 to 20, but the increase from $Y = 20$ to $Y = 25$ does not show any clear change. The shift to lower temperatures with the increase in the carbon to nitrate ratio may be due to decreasing size of the nitrate particles as well as to the interaction between nitrates and carbon.

3.3. Formation of $MnCo_2O_{4+\delta}$

Fig. 7a and b show the IR spectra for the unsupported ($Y = 0$) and supported ($Y = 15$) samples, respectively, heated at temperatures up to 400 °C. The presence of water in the samples is observed from the O–H stretch and bend bands at 3390–3430 and 1590–1630 cm^{-1}. The samples containing nitrates were hygroscopic and exhibit strong bands at these frequencies. The samples where most of the nitrates already had decomposed during the heat treatment were non-hygroscopic. Their water absorptions originate from KBr, which absorbed moisture during the pellet preparation and the measurement, and are shifted to higher frequencies compared to nitrate-containing samples. Compared with the samples without carbon, water bands in the samples containing carbon are slightly shifted to lower frequencies due to formation of C–O–H bonds [19]. Moreover, two additional bands at 1723 and 1242 cm^{-1} are observed for samples containing carbon. These are absorptions from C=O and C–O stretching caused by oxygen functional groups on the surface of carbon [19].

The bands at 825, 1385, and 2427 cm^{-1} in Fig. 7 originate from the presence of nitrates. At 240 °C the intensity of the nitrate band at 1385 cm^{-1} is considerably lower for $Y = 15$ than for $Y = 0$. Part of nitrate ions might be adsorbed on the surface or trapped within the porous structure of the developing oxide [17]. The residual nitrate ions decomposed at lower temperature (below 300 °C) from the supported samples than from the unsupported samples, where the band at 1385 cm^{-1} is observed still at 350 °C.

The adsorption bands around 650–660 and 560–570 cm^{-1} correspond to metal–oxygen stretching in the spinel structure [5,6,20]. For unsupported samples the formation of metal oxide formation is observable not before 240 °C, but for supported samples already around 160 °C. The same was observed in XRD measurements.

The XRD reflections for the supported samples ($Y = 15$) were less intensive and broader than for the unsupported samples. This is still observable in the samples heated at 400 °C (Fig. 8). The sample prepared from the supported nitrates at 400 °C still contained ~18 wt.% carbon as a support for the formed spinel. These observations indicate that the nitrates supported on carbon produce spinel particles with smaller crystallite size than the unsupported nitrates. This can be explained by a confinement effect of the carbon pores: the small pores of the carbon hinder the growth of the crystallised nitrate particles and the forming metal oxides within the pores [1,2].

3.4. Non-stoichiometry

Preparation at low temperatures often produces non-stoichiometric spinel $MnCo_2O_{4+\delta}$ (JCPDS pattern 32–297), which has smaller lattice parameter [7,21,22] than the stoichiometric $MnCo_2O_4$ (JCPDS pattern 23–1237). For example, preparations from nitrates at 400 °C [23] and at 250–500 °C [24], and from citrates and carbonates at 400 °C

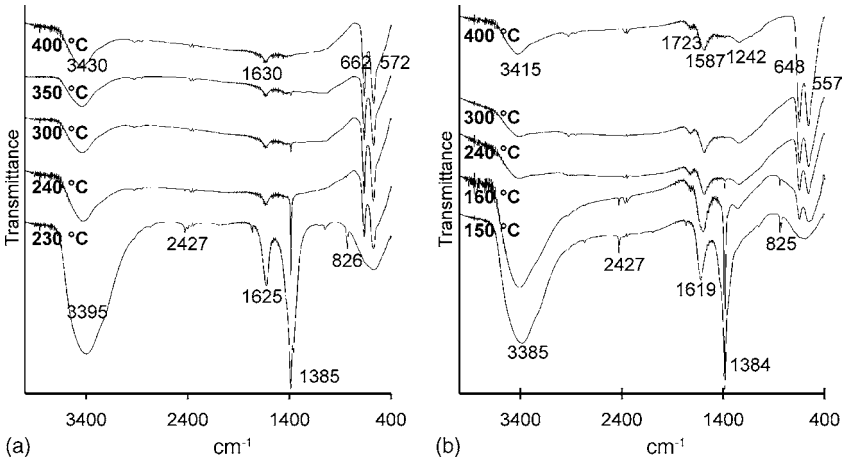

Fig. 7. IR spectra after heat treatments of (a) Mn–Co nitrate ($Y = 0$) and (b) supported Mn–Co nitrate ($Y = 15$).

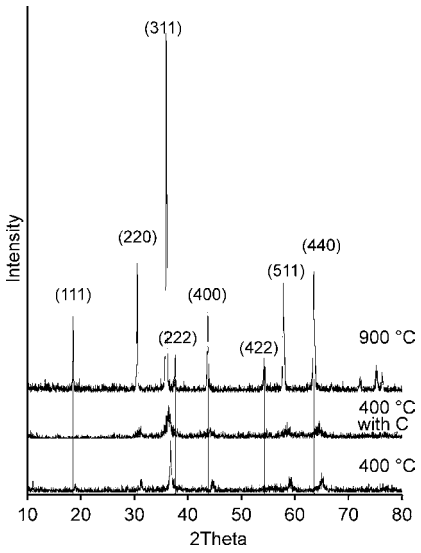

Fig. 8. XRD patterns after heat treatments of (a) Mn–Co nitrate ($Y = 0$) and (b) supported Mn–Co nitrate ($Y = 15$). The vertical lines denote to reflection positions of $MnCo_2O_4$.

[8,22] have produced $MnCo_2O_{4+\delta}$ with $\delta = 0.6$, 0.5–0.3, and 0.6–0.2, respectively. This kind of non-stoichiometry is observed also for $Co_3O_{4+\delta}$ [16]. The cation deficiency possibly induces the existence of OH^- and H_2O groups [23]. The increase in the lattice constant between 300 and 1000 °C is reported to be the consequence of the progressive reduction of Co^{3+} to Co^{2+} and Mn^{4+} to Mn^{3+} [25]. The reduction of Mn^{4+} to Mn^{3+} has also been observed when Mn nitrate was decomposed first into MnO_2, which was reduced into Mn_2O_3 at 500–560 °C [9,13].

For comparison, one sample was prepared at a higher temperature without carbon and its preparation consisted of initial evaporation of water from the aqueous Mn–Co nitrate solutions, decomposition of the nitrates at 250 °C for 2 h, and calcination at 900 °C in air for 8 h. The XRD pattern of this sample (Fig. 8) displays sharp reflections corresponding to $MnCo_2O_4$, and intensive and relatively narrow reflections indicate good crystallinity. The samples heated at temperatures ≤400 °C show lower intensity and broader reflections shifted to higher diffraction angles indicating formation of smaller crystallites of non-stoichiometric $MnCo_2O_{4+\delta}$ [24]. However, the shifting of the reflections is less pronounced in the supported samples. The reflections of the sample prepared by heating the supported nitrates at 160 °C were already at lower diffraction angles than the reflections of the sample prepared from pure nitrates at 240 °C or even at 400 °C. It is probable that the oxidation of carbon has resulted in the reduction of the metal ions and lower non-stoichiometry of the spinel already at relatively low temperatures.

IR measurements showed the metal–oxygen stretching bands at 629 and 543 cm^{-1} for the samples heated at 900 °C. The spinel samples prepared at ≤400 °C (Fig. 7) show shifting of these bands to ∼20 and 30 cm^{-1} higher frequencies for supported ($Y = 15$) and unsupported samples, respectively. Similar shifting of the metal–oxygen absorption bands to higher frequencies has been observed with the decrease of the calcination temperature to prepare $MnCo_2O_4$ [21,26] and with the increase of the oxidation state of metal ions in various metal oxides [20]. This suggests that the oxidation state of the metal ions in the samples prepared in this work increases in the order: preparation at 900 °C < 400 °C from supported nitrates <400 °C from pure nitrates.

To make assessments of the non-stoichiometry, the samples heated at various temperatures were studied by TG-measurements. The samples heated at 900 °C did not lose mass before 1050 °C, where the decomposition of the spinel into MnO and CoO initiated. This indicates that for this sample $\delta = 0$. The sample prepared from pure nitrates at 400 °C started to noticeably lose weight around 460 °C due to gradual removal of oxygen. The calculations showed that the value of δ for this sample was approximately 0.6. Assessment of δ in the samples prepared from the supported nitrates was not possible by TG. The remaining carbon content (∼18 wt.% at 400 °C) could not be measured with sufficient accuracy and the carbon combustion at 300–500 °C occurred simultaneously with the reduction of the metal ions.

Approximations of δ were also done by comparing the positions of reflections (Fig. 8). The reflections of the sample prepared from pure nitrates at 400 °C were fairly close to the reflections of the samples with $\delta = 0.3$–0.5 [24] and 0.6 [23], prepared from nitrates at 270–500 and 400 °C, respectively. Comparison of the reflection positions does not give an exact value of δ, but it still indicates that δ must be higher than 0.3. The reflection positions of the samples prepared from supported nitrates were between the positions of the samples with $\delta = 0.1$ and 0.31 prepared from nitrates at 600 and 500 °C, respectively [24], and thus δ can be assessed to be smaller than 0.3.

The values of δ were also assessed from the TG data of the nitrates and supported nitrates. Because carbon was oxidised up to 450 °C, the value of δ was assessed at 500 °C and was found to be 0.34 for the sample with $Y = 0$ and 0.27 for the sample with $Y = 25$. A clear decrease of δ from these values was observed between 500 and 640 °C for the supported samples and between 570 and 640 °C for the unsupported samples. At 640 °C, δ was calculated to be 0.1 for both samples. These observations indicate that for the unsupported samples the reduction of metal ions occurs mainly between 570 and 640 °C, while for the supported samples the metal ions are partly reduced already during the carbon combustion.

4. Conclusions

The molar ratios of the studied samples were $n(Mn):n(Co):n(NO_3^-):n(C) = 1:2:6:Y$. When mixed Co–Mn nitrates ($Y = 0$) were heated in air, formation of non-stoichiometric spinel $MnCo_2O_{4+\delta}$ was observed at 240 °C. In the case of the supported samples ($Y = 15$) the spinel formation was observed already at 160 °C. Further, the

supported nitrates resulted in a less non-stoichiometric spinel than the pure nitrates. TG-measurements revealed that when carbon content was increased from $Y = 0$ to 20, the onset of the decomposition was shifted to lower temperatures and the decomposition occurred more simultaneously with water evaporation. The increase in the carbon content from $Y = 20$ to 25 did not result in any observable change. The nitrate decomposition was mainly completed at 260–300 °C from the pure nitrates, depending on the heating rate, and 50–70 °C lower temperatures from the supported nitrates. Both the decomposition of nitrates and the spinel oxide facilitated the oxidation of carbon. Vigorous carbon combustion initiated at 260–280 °C, had maximum at 330 °C and ceased after 450 °C.

Acknowledgements

We are indebted to Dr. Ilkka Pitkänen for making the TG–FTIR measurements, and Michael Friman for making the TG–DSC measurements. We thank Nordic Energy Research Program (subprogram Electrochemical Energy Conversion), Fortum Foundation, Wihuri Foundation, and University of Helsinki for financial support.

References

[1] M. Schwickardi, T. Johann, W. Schmidt, F. Schüth, Chem. Mater. 14 (2002) 3913.
[2] M. Ozawa, M. Kimura, J. Mater. Sci. Lett. 9 (4) (1990) 446.
[3] T. Nissinen, Y. Kiros, M. Gasik, M. Leskelä, Chem. Mater. 15 (2003) 4974.
[4] T. Nissinen, Y. Kiros, M. Gasik, M. Lampinen, Mater. Res. Bull. 39 (2004) 1195.
[5] O.V. Sergeeva, A.M. Bol'shakov, G.A. Konin, L.V. Khmelevskaya, Russ. J. Inorg. Chem. 44 (7) (1999) 1045.
[6] G.N. Pirogova, N.M. Panich, R.I. Korosteleva, Yu.V. Voronin, N.N. Popova, Russ. Chem. Bull. 49 (9) (2000) 1536.
[7] A. Restovic, E. Ríos, S. Barbato, J. Ortiz, J.L. Gautier, J. Electroanal. Chem. 522 (2002) 141.
[8] M. Sugawara, M. Ohno, K. Matsuki, J. Mater. Chem. 7 (5) (1997) 833.
[9] P.K. Gallagher, F. Schrey, B. Prescott, Thermochim. Acta 2 (1971) 405.
[10] M. Maneva, N. Petroff, J. Therm. Anal. 36 (1990) 2511.
[11] T. Cseri, S. Békássy, G. Kenessey, G. Liptay, F. Figueras, Thermochim. Acta 288 (1996) 137.
[12] S. Yuvaraj, L. Fan-Yuan, C. Tsong-Huei, Y. Chuin-Tih, J. Phys. Chem. B 107 (2003) 1044.
[13] A.K.H. Nohman, H.M. Ismail, G.A.M. Hussein, J. Anal. Appl. Pyrolysis 34 (1995) 265.
[14] Ž.D. Živković, D.T. Živković, D.B. Grujičić, J. Therm. Anal. 53 (1998) 617.
[15] M.J. Tiernan, E.A. Fesenko, P.A. Barnes, G.M.B. Parkes, M. Ronane, Thermochim. Acta 379 (2001) 163.
[16] M. El Baydi, G. Poillerat, J.-L. Rehspringer, J.L. Gautier, J.-F. Koenig, P. Chartier, J. Solid State Chem. 109 (1994) 281.
[17] S.A.A. Mansour, Mater. Chem. Phys. 36 (1994) 317.
[18] R. Turcotte, R.C. Fouchard, A.-M. Turcotte, D.E.G. Jones, J. Therm. Anal. Calorim. 73 (2003) 105.
[19] R. Schlögl, in: G. Ertl, H. Knözinger, J. Weitkamp (Eds.), Handbook of Heterogeneous Catalysis, VCH Verlagsgesellschaft mbH, Poitiers, 1997, pp. 138–191.
[20] J. Preudhomme, P. Tarte, Spectrochim. Acta 27A (1971) 961.
[21] T.V. Andrushkevich, G.K. Boreskov, V.V. Popovskii, L.M. Plyasova, L.G. Karakchiev, A.A. Ostan'kovich, Kinet. Katal. 9 (6) (1968) 1244 (in Russian).
[22] J.M. Jiménez Mateos, J. Morales, J.L. Tirado, J. Solid State Chem. 82 (1) (1989) 87.
[23] J.L. Gautier, R. Fuentealba, C. Cabezas, Z. Phys. Chem. (Munich) 126 (1) (1981) 71 (in German).
[24] J.-F. Koenig, J. Brenet, C. R. Acad. Sci. B: Sci. Phys. 283 (3) (1976) 71 (in French).
[25] J.L.M. de Vidales, E. Vila, R.M. Rojas, O. Carcía-Martínez, Chem. Mater. 7 (1995) 1716.
[26] Q. Liang, K. Chen, W. Hou, Q. Yan, Appl. Catal. A 166 (1) (1998) 191.